J. CHEM. SOC. FARADAY TRANS., 1994, 90(6), 931–934

FTIR Study of the Interaction of Hydrogen Cyanide with Alkali-metal Ion, Silver(I) and Nickel (II) Ion-exchanged Near-Faujasite Zeolites

Clive J. Blower and Thomas D. Smith*
Chemistry Department Monash University, Clayton, Victoria, Australia 3168

The uptake of hydrogen cyanide by alkali-metal ion-exchanged near-faujasite zeolites involves Lewis acid binding of hydrogen cyanide by the alkali-metal ions such that the —C≡N stretch wavenumber depends on the ionic radii. In the case of lithium and sodium ion-exchanged X and Y zeolite there is a significant formation of characteristic Brønsted acid sites resulting from protonation of the zeolite along with formation of cyanide ion by a reversible process. The uptake of hydrogen cyanide by silver(I) ion-exchanged Y zeolite results in the reversible formation of silver cyanide and zeolite Brønsted acidity. Similar treatment of nickel(II)-exchanged zeolite Y involves Lewis acid complexation of hydrogen cyanide at room temperature and irreversible formation of nickel(II) cyanide within the zeolite at elevated temperatures.

An understanding of the chemical modifications which occur as a result of the occupation of metal ion binding sites of the near-faujasite zeolites X and Y by alkali-metal ions has been achieved by using a diversity of physico-chemical information which focusses attention on their structural features using X-ray and neutron diffraction,[1–4] cation location by ion-exchange[5–7] and carbon monoxide adsorption measurements,[8] dielectric and electrical conductivity,[9,10] far-IR spectroscopy,[11] ^{7}Li NMR,[12] heats of adsorption of water,[13] lattice vibrations,[14] heats of immersion in solutions containing alkenes,[15] and their role in catalysis.[16,17] Various measurements of the basicity of alkali-metal ion-exchanged zeolites have been described, and the importance of the ability of the probe molecule to distinguish between basic and acidic sites as well as exchanged metal ions has been established.[18]

It has been found that the IR spectral measurements of the uptake of hydrogen cyanide by the protonic forms of a number of zeolites are sensitive to the variety of acid sites and structural features of the zeolite.[19] Additionally, hydrogen cyanide meets the criteria required for the detection of basic sites and its potential use in this role is described in the present work.

Experimental

Zeolites Y (Linde SK40) and X, prepared as described previously,[19] were in their sodium ion-exchanged form.

Preparation of Alkali-metal Ion-exchanged Zeolites

To obtain alkali-metal ion-exchanged zeolites, 1.0 g portions of NaY or NaX zeolite were stirred at room temperature for 24 h in 25 cm^3 volumes of the appropriate 99.5% purity alkali-metal ion chloride solution (1 mol dm^{-3}) a total of four times using fresh exchange solution on each occasion. The exchanged zeolite samples were washed thoroughly with distilled water (negative chloride test), air-dried and finally dried at 393 K for 18 h. Storage was over saturated ammonium chloride solution. Exchange of the original NaY and NaX zeolites with sodium chloride solution was conducted to ensure pure NaY and NaX zeolite samples. Exchange levels were determined by atomic absorption spectroscopy and were found to be 100% for lithium and potassium ion-exchanged X and Y zeolites, 70% for RbY and CsY zeolite samples and 78% for RbX and CsX zeolites. These compared well with literature values.[20]

Preparation of Silver, Nickel and Ammonium Ion-exchanged Y Zeolites

AgY zeolite was prepared in darkness by stirring 1.0 g of NaY zeolite in 40 cm^3 of 1.0 mol dm^{-3} silver nitrate solution for 24 h at room temperature followed by three successive exchanges with fresh 40 cm^3 quantities of 0.1 mol dm^{-3} silver nitrate solution for 12 h each. The zeolite product was washed thoroughly with distilled water, air-dried at room temperature and stored in darkness. The level of exchange was 100% according to atomic absorption spectroscopy.

To obtain $N^{(II)}Y$ zeolite with Ni^{2+} ions exchanged into the sodalite cage and hexagonal prism sites,[21] a repetitive exchange–heating cycle was adopted.[22] Hence, 1.0 g of NaY zeolite was stirred in 50 cm^3 of 0.1 mol dm^{-3} nickel nitrate solution for 24 h at room temperature. After filtration and washing, the NiNaY zeolite was heated at 393 K for 2 h, 493 K for 2 h and finally 673 K for 14 h under a stream of nitrogen gas (30 cm^3 min^{-1}). This complete treatment of exchange and heating was repeated. A 90% exchange level was found by atomic absorption spectroscopy.

98% exchanged NH_4Y zeolite, $NH_4(98)Y$, was prepared as described previously.[19]

Hydrogen Cyanide Adsorption Experiments

The procedures for the preparation of hydrogen cyanide and zeolite wafers, adsorption of hydrogen cyanide, recording of the FTIR spectra and data processing (including derivatization) have been detailed previously.[19] Dehydration of wafer forms of metal ion-exchanged X and Y zeolites and deammoniation of the $NH_4(98)Y$ zeolite, to give HY zeolite [H(98)Y], were performed at 593 K for 1 h at 0.001 Torr (prior to hydrogen cyanide adsorption.

2,6-Lutidine (2,6-dimethylpyridine, BDH, i.r.) was dried over sodium hydroxide pellets and distilled (4.11–418 K). Adsorption of 0.50 mmol of 2,6-lutidine onto H(98)Y and NaY zeolites was conducted for 1 h at room temperature in the evacuated cell after wafer dehydration but before hydrogen cyanide adsorption by the normal procedure.

Results

The FTIR spectra in the C≡N stretch region due to hydrogen cyanide adsorbed by lithium-, sodium-, potassium-, rubidium- and caesium-exchanged sodium X, sodium Y zeolite and silver(I)- and nickel(II)-exchanged sodium Y zeolite were recorded. Removal of the less tightly bound hydrogen

cyanide by diminished (0.001 Torr) pressure pumping for 2 min allowed the measurement of the C≡N stretch wavenumber ($\nu_{C\equiv N}$) due to hydrogen cyanide bound to the metal ion centres, as summarized in Table 1. In potassium cyanide the C≡N stretch band occurs at 2078 cm^{-1} and for sodium cyanide at 2092 cm^{-1}.[23]

The uptake of hydrogen cyanide by potassium ion-exchanged zeolite Y results in an IR band due to the —C≡N stretch centred at 2092 cm^{-1} (for simplicity referred to as the 2092 cm^{-1} band) which undergoes some bandwidth reduction on partial removal of hydrogen cyanide at diminished pressure. Spectral derivatization shows that most of the partially removed hydrogen cyanide was bound to Brønsted acid sites on the zeolite framework (2106 and 2114 cm^{-1}), leaving a single band at 2090 cm^{-1} due to hydrogen cyanide bound to exchanged potassium ion. Similarly, for rubidium and caesium ion-exchanged Y zeolite, there is some binding of hydrogen cyanide to Brønsted acid sides, which after pressure desorption shows hydrogen cyanide bound to rubidium ion and caesium ion characterized by spectral bands at 2088 cm^{-1} for RbY and 2082 cm^{-1} for CsY.

The IR spectral bandwidth due to hydrogen cyanide adsorbed onto sodium ion-exchanged zeolite Y shows a much greater IR spectral band narrowing after partial removal of hydrogen cyanide, indicating a greater amount of hydrogen cyanide bound to Brønsted acid sites. Partial removal of hydrogen cyanide leaves that portion bound to exchanged sodium ion characterized by a band at 2101 cm^{-1}.

Since the sodium ion-exchanged zeolite does not possess Brønsted acid sites the interaction with hydrogen cyanide must result in their formation, thus the treatment of sodium Y containing 2,6-lutidine (1601, 1578 cm^{-1}) with hydrogen cyanide results in its conversion to the lutidinium ion (1650, 1678 cm^{-1}). The reversibility of the whole process is demonstrated by the fall in relative intensity of bands due to 2,6-lutidinium ion and rise in the corresponding 2,6-lutidine bands on partial removal of hydrogen cyanide. The other changes brought about by the addition of hydrogen cyanide to silver(I)-exchanged NaY are also reversible, since the bands due to the formation of silver cyanide (2166 cm^{-1}; *cf.* AgCN, 2160 cm^{-1}, $Ag^+(HCN)$, 2138 cm^{-1}, $Ag^+(HCN)_2$, 2147 cm^{-1})[24] along with bands due to hydrogen cyanide at diminished pressure. The IR bands due to hydrogen cyanide adsorbed by the nickel(II) ion-exchanged NaY zeolite, which show little change on pressure reduction, are attributable to hydrogen cyanide bound by nickel(II) (2133 cm^{-1}), Brønsted acid sites (2108 cm^{-1}) and residual sodium ion (2094 cm^{-1}). An increase in temperature (373–573 K) causes a reduction of these band intensities with the appearance of a band at 2172 cm^{-1} due to formation of nickel cyanide [*cf.* nickel(II) cyanide tetrahydrate 2175 cm^{-1}].[25]

The thermal desorption of hydrogen cyanide from alkali-metal ion-exchanged Y zeolite showed that the retention of hydrogen cyanide in each case was greater than that of the protonic form of the zeolite.

Table 1 $\nu_{C\equiv N}$ stretch wavenumbers for HCN adsorbed by metal ion-exchanged zeolites after removal of the less tightly bound HCN at diminished pressures (0.001 Torr); $\nu_{C\equiv N}$ for HCN in the gaseous phase, 2097 cm^{-1}

	$\nu_{C\equiv N}/cm^{-1}$	
metal ion	zeolite Y	zeolite X
Li	2107	2101
Na	2101	2096
K	2090	2082
Rb	2088	2082
Cs	2082	2081
Ag	2108, 2166	—
Ni	2108, 2133	—

Discussion

Ionic Radius Considerations of Hydrogen Cyanide Uptake

X-Ray crystallographic studies of hydrated and dehydrated alkali-metal ion and silver(I) ion-exchanged zeolite Y show that there is a preferential occupation of the hexagonal prisms (site SI)[26] along with exchange into the more accessible sodalite (sites SI*, SII′ and SII_0) and easily accessible supercages (site SII) which contains the greatest number of exchange sites.[27] In the lithium ion-exchanged X zeolite, the lithium ions are located in site SI′ and site SII.[28] The crystal structure of dehydrated nickel(II) ion-exchanged natural faujasite shows that nickel(II) ions occupy two-thirds of the SI sites while the remaining nickel(II) ions are distributed in the region of the SI′, SII′ and SII sites.[29] The nickel(II) ions achieve octahedral coordination in the hexagonal prisms while others have trigonal symmetry in sites SII and SII_0 and in the sodalite sites.[30] As in the case of the uptake of carbon monoxide,[31] metal ions in the hexagonal prisms are inaccessible to hydrogen cyanide. In the uptake of hydrogen cyanide by the various Brønsted acid sites there is a shift of the —C≡N stretch wavenumber to higher values compared to the free-gas value, although there is no clear relationship between the acid strength of each site and the magnitude of the wavenumber shift which may also depend on configurational features of the site symmetry and hydrogen bonding to the nitrogen atom of bound hydrogen cyanide.[19] Again, as in the case for carbon monoxide bonding to metal centres,[31] the increase in IR spectral wavenumber of the —C≡N group compared with that of the free-gas value points to a withdrawal of electron density from the nitrogen atom of the —C≡N group by the hydrogen atom of the Brønsted acid site, leading to a strengthening of the carbon–nitrogen bond. Similar considerations have been made for the interactions of carbon monoxide with zeolite Y in protonic and sodium-exchanged forms.[32]

On the other hand, in circumstances where hydrogen cyanide is bound to an anionic site[33] (*e.g.* $ClHCN^-$, $BrHCN^-$) there is an IR spectral wavenumber shift to values less than that possessed by the free gas, owing to a weakening of the —C≡N bond. As shown in Fig. 1, the binding of hydrogen cyanide to the alkali-metal ion-exchanged zeolites induces an ionic radii-dependent IR spectral shift of the —C≡N band to higher wavenumbers for binding to lithium and sodium ions, compared with the free-gas value, as well as a shift to lower wavenumbers when potassium, rubidium or caesium ions are present. The increase in spectral wavenumber arises from coordination of the hydrogen cyanide by lithium and sodium ions with an orientation of the nitrogen atoms towards the metal ion centre, the strength of the interaction being determined by the ionic radii. The IR spectral shifts to lower values, correlated by a somewhat different slope in Fig. 1, may be thought to arise from an orientation of the hydrogen bond of hydrogen cyanide towards the framework oxide anion of the zeolitic framework, whose effective negative charge depends on shielding by the positive charge on the cation, the effect of which diminishes with increasing cation size.[34]

Existence of Brønsted Acidity in Metal Ion-exchanged Zeolites

Early studies showed that alkali-metal ion-exchanged zeolites X and Y do not possess Brønsted acidity[35,36] while a con-

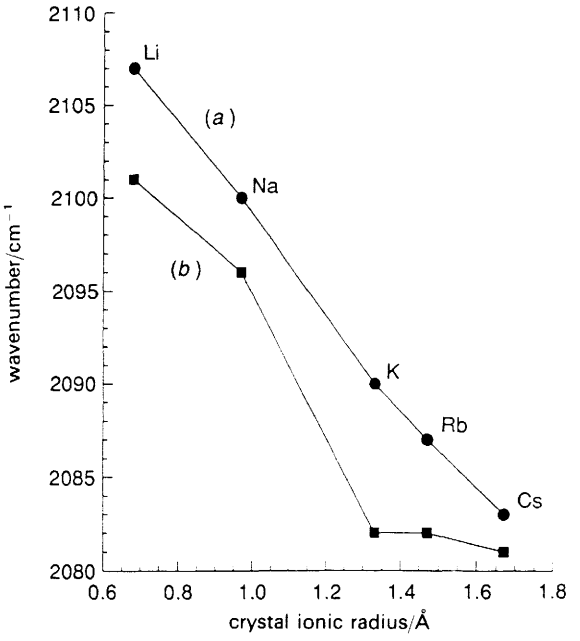

Fig. 1 Change in wavenumber of $\nu_{C\equiv N}$ with alkali-metal crystal ionic radius for hydrogen cyanide adsorbed at room temperature on various alkali-metal ion-exchanged zeolites initially dehydrated at 593 K, after pressure desorption for 2 min at 0.001 Torr: (*a*) Y zeolite, (*b*) X zeolite

temporary study of the time[37] showed that lithium and sodium ion-exchanged zeolites X and Y have significant Brønsted acidity, the presence of which has been used to explain the different products obtained in the alkylation of toluene by formaldehyde on alkali-metal ion-exchanged zeolites X and Y, where the products obtained from the lithium ion-exchanged zeolite catalyst were those expected of acid catalysts.[38] Dissociative adsorption of hydrogen cyanide by silica-supported iron catalysts generates surface hydroxy groups on the silica support,[39] while a similar phenomenon leading to the generation of hydroxy groups has been observed in the adsorption of hydrogen sulfide on zeolite ZSM-5.[40] The Brønsted acidity generated by reversible dissociative adsorption of hydrogen cyanide by alkali-metal ion-exchanged zeolite Y can be measured by the appropriate IR band area due to hydrogen cyanide bound to these sites, excluding the contribution made by the hydrogen cyanide associated with the metal ion centres. A comparison of such areas with that due to hydrogen cyanide adsorbed by zeolite H(98) is shown in Table 2. The greatest level of acidity is found for the lithium ion-exchanged zeolite followed by the silver(I) ion and sodium ion-exchanged forms. Since there is no evidence for the formation of 2,6-lutidinium ion with these metal ion-exchanged forms, it is concluded that these ions take part in dissociative adsorption on subsequent exposure to hydrogen cyanide.

Table 2 Comparison of $\nu_{C\equiv N}$ area, A [using the range 2131–2112 ($\pm$1.5 cm^{-1})] of hydrogen cyanide adsorbed on H(98)Y zeolite with that for alkali-metal ion-exchanged Y zeolites and AgY zeolite, and excluding the HCN bound to the metal ion

zeolite	A/cm^{-1} mg^{-1}	area (%)
H(98)Y	1.39	100
LiY	1.39	100
NaY	0.27	19
KY	0.04	3
RbY	0.07	5
CsY	0.04	3
AgY	1.12	81

Basicity of Alkali-metal Ion-exchanged X and Y Zeolites

It has been shown that the basicity of oxides and alkali-metal ion-exchanged zeolites can be characterized by the IR N—H stretching wavenumber of chemisorbed pyrrole.[41–43] In the case of the alkali-metal ion-exchanged zeolites X and Y, a distinction has been made between the weak acidity of sodium and lithium ion-exchanged zeolite Y and the increasing basicity of potassium, rubidium and caesium ion-exchanged zeolite Y; note that similarly exchanged zeolite X is more basic. The correlation between the N—H wavenumber shifts of pyrrole, using the literature data,[42,43] with those of hydrogen cyanide when adsorbed by alkali-metal ion-exchanged zeolites X and Y is shown in Fig. 2. The wavenumber shifts due to the —C≡N stretch are over a smaller wavenumber range compared with those of the —NH group, in keeping with electronic changes occurring in a multiple bond compared with those in a single bond. However, the correlation of the IR wavenumber shift data for ion-exchanged zeolite Y is good, with both sets of data showing a grouping of lithium and sodium, and potassium, rubidium and caesium on lines of different slopes. The difference is accentuated in the IR wavenumber shift data for alkali-metal ion-exchanged zeolite X which, in addition, shows a more basic character with less effective shielding by the positive charge on the cation. This latter effect is illustrated in Fig. 3, which correlates the literature values of the partial charge on the oxygen of the basic site[42,43] with the IR wavenumber shift of the —C≡N stretch when hydrogen cyanide is taken up by alkali-metal ion-exchanged forms of zeolites X and Y. In both cases, this effect is similar to those shown in correlations of the —NH stretch IR spectral shifts for the chemisorption of pyrrole.[43]

The increased basicity of zeolites which arises as a result of alkali-metal ion exchange may have a profound effect on

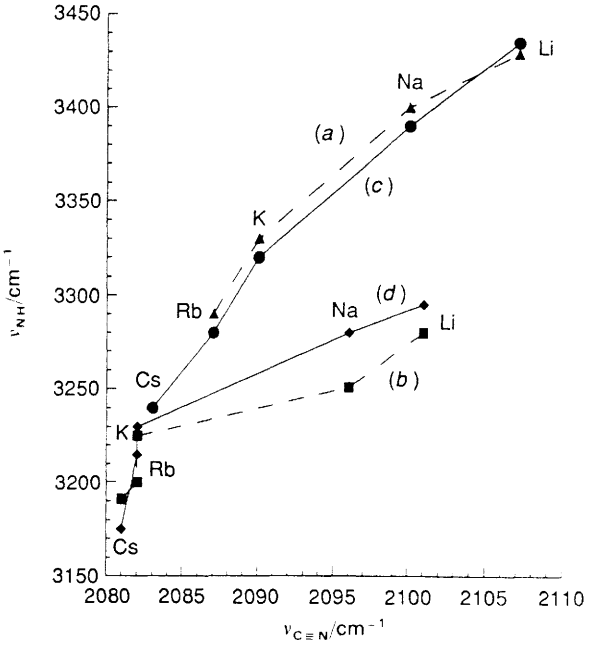

Fig. 2 Comparison of the change in wavenumber of ν_{NH} due to pyrrole adsorbed on alkali-metal ion-exchanged zeolites, with wavenumber of $\nu_{C\equiv N}$ due to hydrogen cyanide pressure-desorbed from similar zeolites initially dehydrated at 593 K. Pyrrole wavenumber data by Barthomeuf:[42] (*a*) Y zeolite, (*b*) X zeolite. Pyrrole wavenumber data by Huang and Kaliaguine:[43] (*c*) Y zeolite, (*d*) X zeolite.

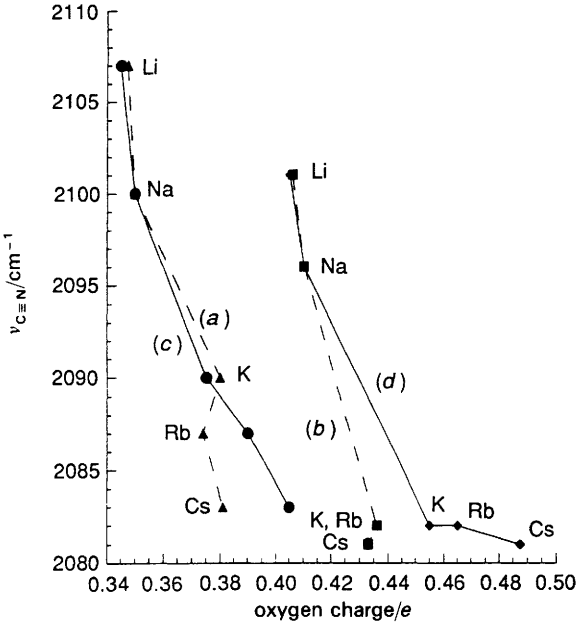

Fig. 3 Comparison of the change in wavenumber of $\nu_{C\equiv N}$, due to hydrogen cyanide adsorbed on alkali-metal ion-exchanged zeolites, with oxygen charge of similar zeolites prepared by Huang and Kaliaguine.[43] Solid lines indicate oxygen charge calculated by approximating the local composition as $Si_{6-n}Al_nO_{12}M_n$ for cation M^+ and dashed lines indicate the calculated oxygen charge of the bulk composition. (*a*) and (*c*), Y zeolite, (*b*) and (*d*), X zeolite.

their catalytic properties. For example, the relative amounts of citronellal and isopulegol formed in an alkali-metal ion-exchanged zeolite X-catalysed Meerwein–Ponndorf–Verley reaction are greatly influenced by the nature of the alkali-metal ion, with the caesium ion favouring the formation of citronellal, and the lithium ion, isopulegol.[44] The results here suggest that the selectivity in product formation may arise from the increased basic character of the zeolite as a result of caesium ion exchange.

References

1 W. J. Mortier, *Compilation of Extra-Framework Sites in Zeolites*, Butterworth, Guildford, 1982.
2 J. V. Smith, *Chem. Rev.*, 1988, **88**, 149.
3 D. W. Breck, *J. Chem. Educ.*, 1964, **41**, 678.
4 L Broussard and D. P. Shoemaker, *J. Am. Chem. Soc.*, 1960 **82**, 1041.
5 P. P. Lai and L. V. C. Rees, *J. Chem. Soc., Faraday Trans. 1*, 1976, **82**, 1809.
6 P. P. Lai and L. V. C. Rees, *J. Chem. Soc., Faraday Trans. 1*, 1976, **72**, 1827.
7 H. S. Sherry, *J. Colloid Interface Sci.*, 1968, **28**, 288.
8 T. S. Egerton and F. S. Stone, *Trans. Faraday Soc.*, 1970, **66**, 2364.
9 D. Vucelic, *J. Chem. Phys.*, 1977, **66**, 43.
10 R. A. Schoonheydt and J. B. Uytterhoeven, in *Molecular Sieve Zeolites 1*, ed. R. F. Gould, *Adv. Chem. Ser. 101* Am. Chem. Soc., Washington D.C., 1971, p. 456.
11 W. M. Butler, C. L. Angell, W. McAllister and W. M. Risen, *J. Phys. Chem.*, 1977, **81**, 2061.
12 H. Herden, W.-D. Einicke, R. Schöllner and A. Dyer, *J. Inorg. Nucl. Chem.*, 1981, **43**, 2533.
13 O. M. Dzhigit, A. V. Kiselev, K. N. Mikos, G. G. Muttik and T. A. Rahmanova, *J. Chem. Soc., Faraday Trans. 1*, 1971, **67**, 458.
14 V. M. Radak, T. S. Cerancic and I. M. Zivadinovic, *Z. Naturforsch., Teil B*, 1978, **33**, 1116.
15 H. Herden, W-D. Einicke, V. Messow, K. Quitzsch and R. Schöllner, *J. Colloid Interface Sci.*, 1984, **97**, 565.
16 P. B. Venuto and P. S. Landis, *Adv. Catal.*, 1968, **18**, 259.
17 P. E. Hathaway and M. E. Davis, *J. Catal.*, 1989, **116**, 263.
18 D. Barthomeuf, G. Coudurier and J. C. Vedrine, *Mater. Chem. Phys.*, 1988, **18**, 553.
19 C. J. Blower and T. D. Smith, *J. Chem. Soc., Faraday Trans.*, 1994, **90**, 919.
20 H. S. Sherry, *J. Phys. Chem.*, 1966, **70**, 1158.
21 P. Gallezot and B. Imelik, *J. Phys. Chem.*, 1973, **77**, 652.
22 A. Dyer and R. P. Townsend, *J. Inorg. Nucl. Chem.*, 1973, **35**, 2993.
23 Z. K. Ismail, R. H. Hauge and J. L. Margrave, *Appl. Spectrosc.*, 1973, **27**, 93.
24 M. F. A. Dove and J. G. Hallett, *J. Chem. Soc. A*, 1969, 2781.
25 R. A. Nyquist and R. O. Kagel, *Infrared Spectra of Inorganic Compounds*, Academic Press, New York, 1971, p. 61
26 J. V. Smith, J. M. Bennett and E. M. Flanigen, *Nature (London)*, 1967, **215**, 241.
27 G. R. Eulenberger, D. P. Shoemaker and J. G. Keil, *J. Phys. Chem.*, 1967, **71**, 1812.
28 Yu. F. Shepelev, A. A. Anderson and Yu. I. Smolin, *Zeolites*, 1990, **10**, 61.
29 D. H. Olson, *J. Phys. Chem.*, 1968, **72**, 4366.
30 T. A. Egerton and F. S. Stone, *J. Chem. Soc., Faraday Trans. 1*, 1973, **69**, 39.
31 T. A. Egerton and F. S. Stone, *J. Chem. Soc., Faraday Trans. 1*, 1973, **69**, 22.
32 S. Beran, *J. Phys. Chem.*, 1983, **87**, 55.
33 J. A. Salthouse and T. C. Waddington, *J. Inorg. Nucl. Chem.*, 1978, **40**, 1696.
34 M. J. Edgell, R. W. Paynter, S. C. Mugford and J. E. Castle, *Zeolites*, 1990, **10**, 51.
35 J. W. Ward, *J. Catal.*, 1968, **10**, 34.
36 J. W. Ward, *J. Catal.*, 1969, **14**, 365.
37 Y. Watanabe and H. W. Habgood, *J. Phys. Chem.*, 1968, **72**, 3066.
38 T. Yashima, K. Sato, T. Hayasaka and N. Hara, *J. Catal.*, 1972, **26**, 303.
39 C. Johnston, N. Jorgensen and C. H. Rochester, *J. Chem. Soc., Faraday Trans. 1*, 1988, **84**, 3605.
40 C. L. Garcia and J. A. Lercher, *J. Phys. Chem.*, 1992, **96**, 2230.
41 P. O. Scokart and P. G. Rouxhet, *J. Chem. Soc., Faraday Trans. 1*, 1980, **76**, 1476.
42 D. Barthomeuf, *J. Phys. Chem.*, 1984, **88**, 42.
43 M. Huang and S. Kaliaguine, *J. Chem. Soc., Faraday Trans.*, 1992, **88**, 751.
44 J. Shabtai, R. Lazar and E. Biron, *J. Mol. Catal.*, 1984, **27**, 35.

Paper 3/03774F; *Received* 30*th June*, 1993